EXPERIMENTAL AND ANALYTICAL STUDY OF FLASHING FLOW THROUGH STEAM GENERATOR TUBE CRACKS

Shripad T. Revankar
School of Nuclear Engineering
Purdue University and POSTECH
School of Nuclear Engineering, West Lafayette, IN 47907 USA
shripad@purdue.edu

Jovica R. Riznic
Canadian Nuclear Safety Commission
280 Slater, P.O.B. 1046, Station B, Ottawa, ON, Canada
Jovica.riznic@cnsc-ccsn.gc.ca

ABSTRACT

In the present study an experimental program and analysis methods were developed to measure and assess the choking flow rate of subcooled water through simulated steam generator tube crack geometries. Experiments were conducted on choking flow for various simulated crack geometries for vessel pressures up to 7 MPa with various subcoolings. Measurements were done on subcooled flashing flow rate through well-defined simulated crack geometries with L/D<5.5. Both homogeneous equilibrium and non-equilibrium mechanistic models were developed to model two-phase choking flow through slits. A comparison of the model results with experimental data shows that the homogeneous equilibrium based models grossly under predict choking flow rates in such geometries, while homogeneous non-equilibrium models greatly increase the accuracy of the predictions.

KEYWORDS
Steam generator tube cracks, leak before break, flashing flow, choking flow, experiments and model,

1. INTRODUCTION

Steam generator (SG) tubes have an important safety role because they constitute one of the primary barriers between the radioactive and non-radioactive sides of the both CANDU reactors and Pressurized Water Reactors (PWR) plants. Thus integrity of SG tubes is a safety-related issue, since the tubes are susceptible to corrosion and damage. There are many identified degradation mechanisms related to SG tubes which include; intergranular attack and outside diameter stress corrosion cracking (SCC), primary water stress corrosion cracking, tube fretting and wear, foreign material wear, pitting, high cycle fatigue, and wastage or thinning. The ability to estimate the leak rates from the through wall cracks in the steam generator tube is important in terms of radiological source terms and overall operational management of steam generators as well as demonstration of the leak-before-break condition. Traditionally, steam generators and steam generator tubes were designed with a sufficient safety margin against rupture. The design requirements of ASME code and the Nuclear Regulatory Commission (NRC) for steam generator tubes for continued operation under main steam line break (MSLB) is $1.4\Delta P_{MSLB} > 25$ MPa [1]. These safety margins are based on the rupture or burst pressure of an unflawed tube. A typical unflawed Alloy 600 tube has an industry expected burst pressure of ~86 MPa [2]. Steam generator operability requires the completion of steam generator tube inspections using non-destructive techniques, usually eddy current examination, in intervals ranging from 12 to 40 months.

There are also further steam generator tube integrity assessment guidelines which provide assessment procedures and criteria for assessing tube integrity for burst/collapse and through wall leakage, loading definitions, and design margins [3]. The final result is that steam generators operate under the leak-before-break concept, which demonstrates that a crack can grow through-wall, resulting in a leak, and that this through-wall flaw will be detected by leakage monitoring systems well before the flaw becomes unstable and the tube ruptures. Much research in the area of steam generator tube integrity is therefore related to the burst characterization of tubes with flaws [4]. Literature survey shows that most of the data on simulated steam generator cracks is carried out with the tube ultimately leading to burst [5]. The break geometry characterization is not properly carried out to associate the discharge data with a well characterized break. Thus prediction and benchmarking the predictions of leak rates through SG cracks with data is challenging.

There is very limited data on the steam generator tube leak rate measurement. Most studies of subcooled choking flow are related to long tubes with large *L/D* (*L*= channel length and *D*= crack hydraulic diameter) and nozzles [6-9]. A literature survey lists the limited sets of data that focus on crack and simulated crack geometries. The survey shows that this geometry has been studied over a large range of pressures and liquid subcoolings however, as can be seen, these data focus on *L/D* geometries greater than 15. Also, all of those data have a channel length greater than 10 mm, which is not indicative of steam generator tubing. Steam generator tubes have a wall thickness typically less than 3 mm. In view of this an experimental program was carried out where the simulated steam generator tube crack geometry was well characterized and choking flow of subcooled water tests were performed

2. EXPERIMENTAL PROGRAM

Design of a test facility to measure leak rates of through wall cracks was based on the following goals. (1) The test facility should be modular so that various crack geometries can be studied. (2) The pressure differential across the break should be similar to the prototype about 6.8 MPa (1000 psi). (3) Facility should be such that tests can be easily repeated. Based on these goals a test facility is designed. Figure 1 shows a schematic of the test facility design. It consists of a vertical pressure vessel, which serve as the blowdown tank, a water tank where steam condenses and the discharge from crack is collected and measured, a nitrogen supply line to pressurize the vessel with control valve, instrumentation and data acquisition system.

2.1 Blowdown Vessel

The volume of the vessel was based on the maximum discharge rate expected from the crack. In designing the test facility the most important aspect is the volume of the pressure vessel as this will determine what leak rates can be measured and for how long. Also, the size of the condensing tank will affect this as well. The pressure vessel was constructed from a single 3.5 inch diameter schedule 160 and 316SS seamless pipe. It is 3.05 m in length and has numerous inlet and outlet ports including a 1 inch NPT port for connection to the test section specimens and ¼ inch ports for pressure measurement and thermocouples. The flow cross section areas for cracks are in the order of 10^{-7} m^2 to 10^{-6} m^2. The discharge section cross section is 2×10^{-3} m^2. So the ratio of areas between the two is 10^3, thus the effect of the confined geometry is negligible on the discharge flow. It should be noted that the back pressure is key for critical pressure –as long as it is less than half of the upstream condition choking occurs.

The vessel is equipped with one pressure relief valve with manufacturer preset of 8.3 MPa. The pressure vessel is pressurized using compressed nitrogen bottles connected via 3/8 inch SS tubing. A single stage regulator with downstream pressure gauge range of 0-13.8 MPa is used to keep a constant regulated pressure during a given experimental run. Due to the high pressure and temperature at the extreme end of the range of experiments performed, submersible type heaters were not able to be used. The vessel water was heated from outside the pressure vessel using three band heaters 3 inches wide with and I.D. of 4.5 inches. The band heaters are Watlow® brand thin band ceramic insulated heaters. Each heater is capable of producing 1200 Watts and run in parallel off a 240 volt power supply. The entire pressure vessel and piping to the test section are insulated with 2 inches of mineral wool variety insulation.

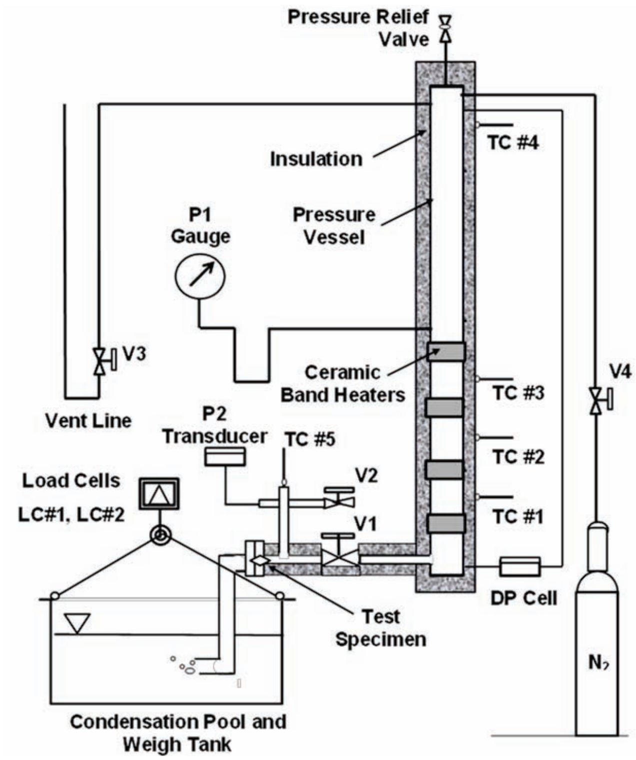

Figure1. Schematic of Test Facility

2.2 Pressure and Temperature Measurement

One differential pressure transducer and one gauge pressure transmitter are used for pressure data acquisition. The differential pressure transducer is a Honeywell ST3000® smart transducer used to measure the water level in the pressure vessel. A gauge pressure transmitter, located at P2 in Fig. 1 is used to measure the pressure just before the choking plane. The transmitter was manufactured and calibrated by Ashcroft®, with a range of 0-13.8 MPa with accuracy of 1.0%. Other pressure measurements are also available through needle gauges. As stated above, there is a pressure gauge on the nitrogen regulator. Also, a WIKA® brand needle gauge with a range of 0-6.9 MPa is located at P1. This allows for redundant monitoring of the vessel pressure.

Temperatures were measured using 5 K-type stainless steel sheathed thermocouples at locations T1-T5. Measurements were taken at a rate of 1 Hz. At TC5 a tee was used to allow both pressure and temperature to be measured at the same location just upstream of the test section break. All thermocouples were inserted to the center-line of the flow at their respective locations.

2.3 Discharge Rate Measurement

A 25.4 cm bolted bonnet full port gate valve initiates the experiment and the steam produced in the test section break is piped to the weigh tank where it is condensed. This allows for the dynamic measurement of the mass of water in the weigh tank. The following describes the components involved in this measurement. A 189.3 liter condensing tank is suspended from two high precision miniature load cells via steel cable at LC1 and LC2. The load cells work in both tension and compression and have a load capacity of 136.07 kg each. Both were manufacturer calibrated and in-house calibrated. Their full scale output is different for each, but is approximately 2.2 mV/V with a combined error of less than 0.1%. Over a 20 minute period their full scale creep is less than 0.05%. In order to increase the accuracy of the load cell data acquisition, a signal amplifier is used to amplify the signal before being recorded. All electronic components are allowed to warm up a sufficient amount of time before an experiment was conducted.

2.3 Data Acquisition System

Two separate data acquisition boards made by Measurement Computing® were used for data acquisition. A PCI-DAS-TC board was used for thermocouple measurement. This board allows for 16 differential thermocouple input channels, with a resolution of 0.03 degrees C. The other board was used for the pressure transmitter, load cells, and differential pressure transducer. This board, a PCIM-DAS16JR/16 can handle up to 16 single ended or 8 differential analog inputs with 16 bit resolution. All data acquisition was streamed through and collected using a program written in Lab VIEW® software. Thermocouple data was taken at 1 Hz while all other data was taken at 20 Hz.

3. TEST SPECIMENS

For obvious reasons, there are a limited number of actual steam generator tube cracks that are available for use in any experimental program. Cracked tubes that are removed from service have been studied by a limited number of groups [5, 10, 11]. These limited studies however use destructive examination and experimental techniques to establish modes of failure for the tubes with flaws. Actual tube flaws can vary in size (microscopic to macroscopic), shape, location, and roughness depending on the flaw type and morphology while in service. The flaws themselves are affected by the length of time they are in service, corrosion, vibrations and stress, as well as thermal-hydraulic conditions. This makes it difficult to study actual tube flaws in a laboratory environment, where many tests can be conducted under well controlled conditions. It is very difficult to reproduce crack-like flaws whether they are very tight, deep, corrosion, or pitting type.

Two types of test specimens were used in the experimental program. One type laser cut rectangular slit with crack channel length of 1.3 mm and L/D = 2.0 to 2.1. The other type was made by welding two plates had crack channel length of 1.3 mm and L/D from 1.3 – 2.1. Table 1 shows the test specimen geometry. The laser cut slit test specimens with channel length of 3.1 mm are numbered as 1, 2 and 3 while the welded samples are number as 4, 5, 6 and 7 respectively. Slit test specimen #2 is shown in Figure 2. The laser cut method cannot produce a uniform cross section through the depth of the cut due to melting effects in the material. Therefore, one side of the cut will have a slightly different area than the other. The effective cross sectional flow area was calculated by averaging the front and back cross sections of the slits. The channel surfaces for laser cut specimen were rough while that for weld specimen were smooth. In Figure 3, the weld specimen #5 is shown.

4. TEST RESULTS

4.1 Cold Water Discharge Tests

Flow discharge tests were carried out with water at room temperature (20^{o}C). Since the water is discharged to atmospheric pressure, the upstream pressure represents total pressure drop across the slit. Using the flow rate data the Reynolds number *Re*, and the discharge coefficient C_d for the slit are calculated. The data on discharge coefficient as a function of pressure showed that a square root fit to the pressure showing that in both cases the mass flux increases as a square root of pressure. The discharge coefficient for slit #2 it varies from 0.51 to 0.75 and for slit #5 it varies from 0.65 to 0.83.

Table 1. Sample Slit Specimen Geometry

Sample #	Type	Area [m²]	Hydraulic Diameter D_h [m]	Channel Length L [m]	L/D_h
1	Laser cut	9.060E-07	6.220E-04	1.300E-03	2.1
2	Laser cut	5.769E-07	6.355E-04	1.300E-03	2.0
3	Laser cut	4.639E-07	6.172E-04	1.300E-03	2.1
4	Weld	1.404E-06	9.755E-04	1.300E-03	1.3
5	Weld	4.594E-06	1.043E-03	1.300E-03	1.2
6	Weld	1.110E-06	6.214E-04	1.300E-03	2.1
7	Weld	5.132E-07	7.483E-04	1.300E-03	1.7

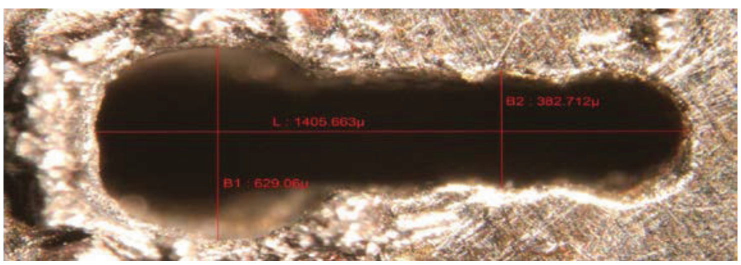

Figure 2. Laser cut specimen # 2 with L/D 2.1

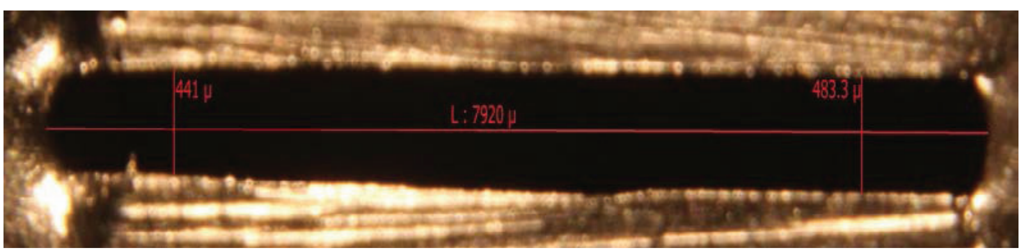

Figure 3. Weld specimen # 5 with L/D 1.2

4.2 Subcooled Flashing Discharge Tests

Tests of flashing choked flow with heated water were carried out up to a vessel pressure of 6.89 MPa (1000 psi). As the experimental program was designed for testing choking flow through steam generator tube cracks, the most valuable data are those at the highest pressures. The tests carried out at approximately 6.89 MPa, have a pressure differential across the choking plane of near equal value.

The tests carried out were varied with subcooling at near the same pressures. Pressures for the tests ranged from 6.87 MPa to 6.60 MPa, with a range of subcooling between 51.4 ^{o}C and 24.7 ^{o}C. The highest mass flux for each specimen was obtained at the highest subcoolings, along with the lowest mass flux for the lowest subcoolings as expected. The tests carried out for slit specimen #2 at various pressures and subcooling of 25 ^{o}C. The heated water flashes as it is discharged from the cracks and hence the mass flux discharge decreases with the heated tests. The comparison between cold water tests discharge and heated tests discharge for slit #2 can be seen in Figure 4 as a function of pressure. A representation of the mass flux data with respect to subcooling can be seen in Figure 5. As the subcooling increases for each specimen the mass flux increases. The mass flux varies with channel area and the variations in mass flux are due to channel roughness.

4.3 Experimental Uncertainty Analysis

Experimental data uncertainty analysis was carried out for measured data such as, diameter, pressure temperatures, and mass of the discharged water using instrument measurement uncertainties, and for the uncertainties in calculated parameters such as mass flux, error propagation method was employed. The total relative error in the mass flux data using the weight tank measurement method ranged from 1.17 % to 1.95 % for all experimental runs. Errors for a representative case are shown in Table 2. The error contributions from the different parameters of interest for the same run are shown in Table 3.

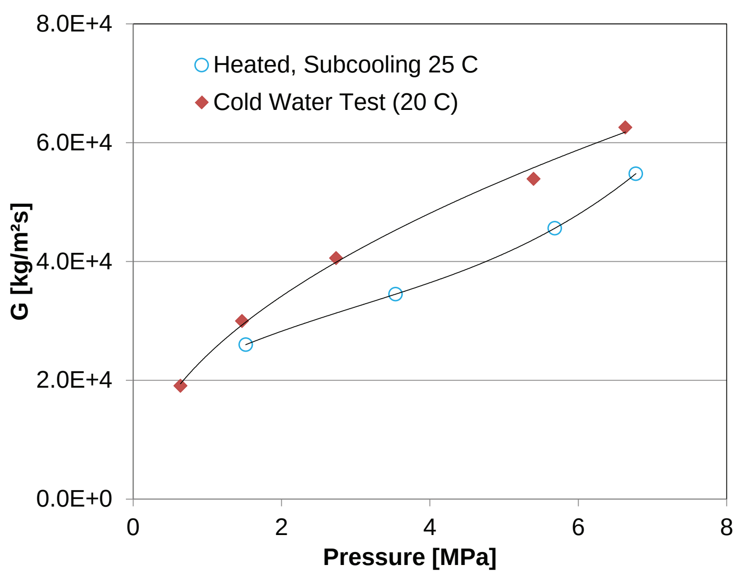

Figure 4.Cold water discharge mass flux and subcooled flashing mass flux for laser cut slit # 2

5. CHOKING FLOW MODELS

5.1 Homogeneous Equilibrium Model

The choking flow in the slit was modeled using homogenous equilibrium model (HEM) and homogenous non-equilibrium model (HNEM). Both single phase flow and two-phase flow may occur in the subcooled flashing flow in slit. Depending on the subcooling, the fluid may flash at the entrance of the crack or in the channel itself. The flow in the slit channel may start as single phase flow and then flash into two phase flow downstream the channel or at exit. A one-dimensional model for two-phase choking flow was developed [12]. A reservoir contains a fluid at constant pressure P_0 and temperature T_0 called the stagnation state. If the back pressure P_b is equal to P_0 then obviously no flow will occur in the channel. As P_b decreases, flow begins and a pressure gradient is established along the channel. Also, as P_b

decreases, the flow rate increases until the back pressure reaches a critical pressure. At this point choking flow is obtained and any reduction in P_b beyond P_c does not change the flow rate or the pressure gradient in the channel. If the stagnation state is at saturation, then the entrance loss of the channel will cause the fluid to flash at the entrance. In this case, the channel only contains a two-phase mixture. In the case of higher subcooling, flashing will occur somewhere along the length of the channel.

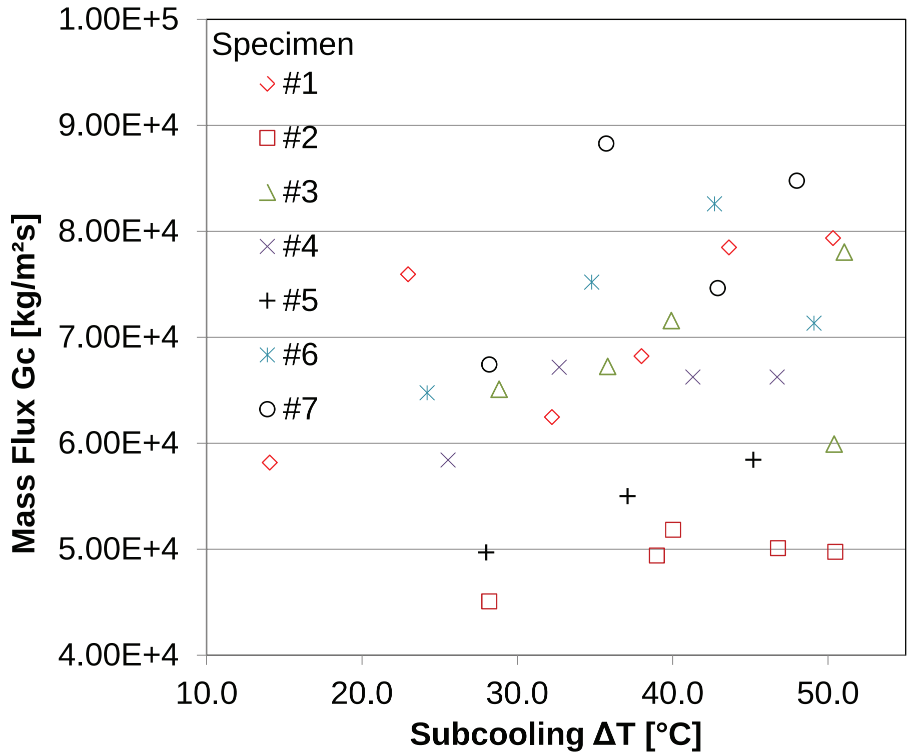

Figure 5. Choking flow for specimens slit#1- slit#7 at 7 MPa

Table 2. Error for a representative test case, P = 6.7277 MPa, G=6.5707X10^4 kg/m^{2}s

Parameter	Value (1)	Standard Error (2)	Relative Error (2)/(1)
Mass flux G (kg/m2s)	65707.5	1279.3	0.01947
Pressure P (Pa)	6727738	67277.38	0.01
Temperature T (^{o}C)	237.04	1	0.0042

Table 3. Error contribution for a representative case

Parameter	Standard Error	Error Contribution		
Mass flux G, (kg/m2s)	1279.3	Mass 1 (kg)	Mass 2 (kg)	Area (m2)
		456.627	465.627	314.572

If one considers flashing to begin when the fluid reaches saturation, then flashing will occur at the point along the channel where the pressure drops below the corresponding saturation pressure at the stagnation temperature T_0. This is consistent with a homogeneous equilibrium model. This pressure drop is attributed to the single phase liquid frictional pressure drop along the channel. The main HEM assumption is that the two fluids are in thermodynamic equilibrium, which takes the dependent variable T out of the equation set. However, quality has now been introduced as a dependent variable via the state equations.

The governing equations of mass, momentum and energy equations for HEM are available from [12] and are not given here to save space.

Flashing Criteria

The upstream boundary conditions for the HEM mixture are given by the solution of the liquid flow equations at the point where flashing occurs. The flashing criterion for the HEM is: $P_{fl} = P_{sat}(T)$. This is close to the Lackmé's [13] proposed flashing criterion: $P_{fl} = k_1 P_{sat}(T)$, where k_1 =0.95. Therefore the boundary condition for the HEM equations is: $P(z_{fl}) = P_{sat}(T)$. From the liquid equations we have, $u(z_{fl}) = u(z_{fl})$, $x(z_{fl}) = 0$, $h(z_{fl}) = h_{fl}$, where the subscript *fl* represents the location of flashing.

Choking Flow Criteria

Applying the assumptions of the HEM to sound speed criteria, the critical velocity of the fluid is derived as,

$$u_c = a_{HE} = v\left[-\left((1-x)\frac{dv_f}{dP} + x\frac{dv_g}{dP} + v_{fg}\left(\frac{dx}{dP}\right)_s\right)\right]^{-1/2} \tag{1}$$

The equilibrium mass transfer rate for an isentropic process is obtained by taking the derivative of quality with respect to pressure at saturation given in equation (2):

$$\left(\frac{dx}{dP}\right)_s = \frac{(1-x)\dfrac{ds_f}{dP} - x\dfrac{ds_g}{dP}}{s_{fg}} \tag{2}$$

The solution procedure is terminated once the mixture velocity is equal to the critical velocity given in equation (1). Supersonic choking is assumed to occur if the liquid velocity is greater than the zero quality sound speed. If this occurs, flashing and choking both occur at the exit plane. The zero quality sound speed is evaluated by simply taking x = 0 in equations (1) and (2).

5.2 Homogeneous Non-Equilibrium Model (HNEM)

A second modeling approach is derived below, which accounts for two-phase flow in non-equilibrium, where the fluid phase is allowed to become superheated and the vapor phase is assumed to follow the saturation curve. The amount of liquid superheat required for flashing is determined by the use of the pressure undershoots correlation based on that of Alamgir and Lienhard [14]. Applying this assumption along with mixture properties to the single phase equations allows the derivation of the HNEM to be carried out. Here, derivatives of liquid properties with respect to temperature cannot be neglected. The chosen dependent variables are thus, pressure (*P*), mixture velocity (*u*), liquid temperature (T_l), and thermodynamic quality (*x*). For completeness, a more detailed derivation is carried out for this model starting with the single-phase conservation equations.

The mass conservation equation is given by

$$-\frac{1}{v}\left[(1-x)\left(\frac{\partial v_l}{\partial P}\right)_T + x\frac{dv_g}{dP}\right]\frac{dP}{dz} - \frac{1}{v}(1-x)\left(\frac{\partial v_l}{\partial T_l}\right)_P\frac{dT_l}{dz} - \frac{(v_g - v_l)}{v}\frac{dx}{dz} + \frac{1}{u}\frac{du}{dz} = 0 \tag{3}$$

The momentum equation is much more simple, however since two phases (liquid and vapor) are now being considered, two-phase frictional pressure drop must be accounted for. Levy [15] proposed a simple approximation to the Lockhart-Martinelli correlation for two-phase frictional pressure drop using the single phase friction factor *f*. This relationship is adopted in this study, and is given as:

$$\left(\frac{dP}{dz}\right)_f = \frac{1}{(1-\alpha)^2} f \frac{\left[G(1-x)\right]^2 \nu_l}{2D_h} \tag{4}$$

Since this approximation involves void fraction, it is necessary to relate the void fraction to the steam quality *x*. For a homogeneous mixture we have,

$$\alpha = \frac{1}{1+\left(\frac{1-x}{x}\right)\frac{\nu_f}{\nu_g}} \tag{5}$$

Using these relations, the momentum equation below can now be solved for the homogeneous non-equilibrium mixture as:

$$\frac{dP}{dz} = -\left(\frac{dP}{dz}\right)_f - \frac{u}{\nu}\frac{du}{dz} \tag{6}$$

Using mixture properties:

$$h = (1-x)h_l + xh_g \text{ or } h = f(x, h_l, h_g) \tag{7}$$

And assuming liquid is in non-equilibrium (superheated) with saturated vapor:

$$h_l = f(P,T) \text{ or } h_g = f(P)_{sat} \tag{8}$$

then the energy equation is given as:

$$\left[(1-x)\left(\frac{dh_l}{dP}\right)_T + x\frac{dh_g}{dP}\right]\frac{dP}{dz} + u\frac{du}{dz} + (1-x)\left(\frac{dh_l}{dT}\right)_P \frac{dT_l}{dz} + (h_g - h_l)\frac{dx}{dz} = 0 \tag{9}$$

Equations (3), (4), and (9) can now be used to solve for *P*, *u*, and *x*. A fourth equation however is required to solve for the fourth unknown dependent variable i.e., the liquid superheat T_l. A common method of determining the liquid temperature in non-equilibrium flows is to use a relaxation to equilibrium method. A simple exponential relaxation model is chosen in this work, however it should be noted that with better information about vapor generation, future modeling efforts might employ a more specific relaxation method that correlates well with adiabatic two-phase flow in short channels. The exponential relaxation to equilibrium was proposed by Bauer et al. [16]. Applying an exponential relaxation to the pressure undershoot at flashing allows for a correlation for the liquid superheat to take the following form [17]:

$$\frac{dP}{dz} = \left(\frac{dP}{dT_l}\right)_{sat} \frac{dT_l}{dz} + \frac{d(\Delta P_{fl})}{dz} \exp\left(\frac{-\tau_r}{\tau'}\right) \tag{10}$$

where τ' is a parameter of the model that determines the rate at which the two-phase mixture relaxes to equilibrium and τ_r is the residence time of the two-phase mixture after flashing inception in the channel. The equation (10) is a profile-fit-type equation for liquid superheat. Residence time is given by:

$$\tau_r(z) = \int_{z_{fl}}^{z} \frac{dz'}{u(z')} \tag{11}$$

The superheat required for vapor generation is given in terms of a pressure undershoot below saturation pressure (ΔP_{fl}).

$$P_{fl} = P_{sat} - \Delta P_{fl} \tag{12}$$

The pressure undershoot chosen was a modification by Levy and Abdollahian [18] to that of Alamgir and Lienhard [14] correlation for choking flow in large and small scale experiments given as :

$$\Delta P_{fl} = \frac{0.258\sigma^{1.5} T_r^{13.76} (0.49 + 13.25\Sigma^{0.8})^{0.5}}{(k_s T_c)^{0.5}\left(1 - \frac{\nu_f}{\nu_g}\right)} \tag{13}$$

where T_c = critical temperature (K), T_i = initial temperature in a depressurization process (K), $T_r = T_i/T_c$ = reduced temperature , Σ = the rate of depressurization (Matm/s), σ = surface tension between liquid and vapor (N/m), and k_s = Boltzmann's constant (J/K).

Flashing Criteria

The flashing criteria for the HNEM is given in terms of the pressure undershoot beyond saturation pressure given by equation (12). This is consistent with a thermal non-equilibrium assumption. The pressure undershoot allows for the liquid to become superheated beyond the saturation temperature at the fluid pressure in order for vaporization to occur. This correlation was developed based on, and supported by, direct experimental evidence. While simple, the correlation was based on static depressurization of subcooled fluid.

Critical Flow Criteria

As with the HEM a speed of sound criteria is required for critical flow for HNEM that is consistent with the assumptions used. Kaizerman et al. [19] have proposed a speed of sound by performing characteristic analysis on inhomogeneous non-equilibrium two-phase flow using the drift-flux model. A formulation for homogeneous flow in which the vapor phase is assumed to be saturated and the liquid phase in non-equilibrium is adopted for this model. For the case of zero drift-flux, the resulting expression is given as:

$$u_a = \left[\rho_m\left(\frac{(R_H)_l}{\rho_l^2} + \rho_m E\right)\right]^{-1/2} \tag{14}$$

where E is given as:

$$E = c\left[\frac{1}{\rho_g^2}\frac{d\rho_g}{dP} - \frac{1}{\rho_l^2}(R_H)_l\frac{dh_g}{dP}\right] + (1-c)\frac{(R_p)_l}{\rho_l^2} \tag{15}$$

and c is the mass concentration of the vapor phase and is equivalent to: $c \equiv \alpha\rho_v / \rho_m$, and R_H and R_P are defined for the liquid phase as:

$$(R_H)_l = \left(\frac{\partial\rho_l}{\partial h}\right)_P, \quad (R_P)_l = \left(\frac{\partial\rho_l}{\partial P}\right)_h \tag{16}$$

6. CHOKING FLOW MODEL RESULTS

6.1 HEM Model Results

The model implementation was carried over to the data from the current experimental program. The choking mass flux data measured for all slits #1-7 are compared in Figure 6 with the HEM predictions. For a much smaller channel length (1.3 mm) as characteristic to the current tests the HEM significantly under-predicts the critical mass flux. Unfortunately, unlike previous studies on longer channels L/D > 20) , it is not possible to place pressure taps along such a short channel to obtain pressure profile data or estimate the exit pressure along the channel. Also, there is not a large enough database as of yet, to make formal conclusions about the effect of L on the model predictions, however from these limited data sets, the HEM predictions were lower than -20%, of the experimental data for simulated SG tube cracks as shown in Figure 6. Some predictions were lower than experimental data as much as 27% from experimental data..

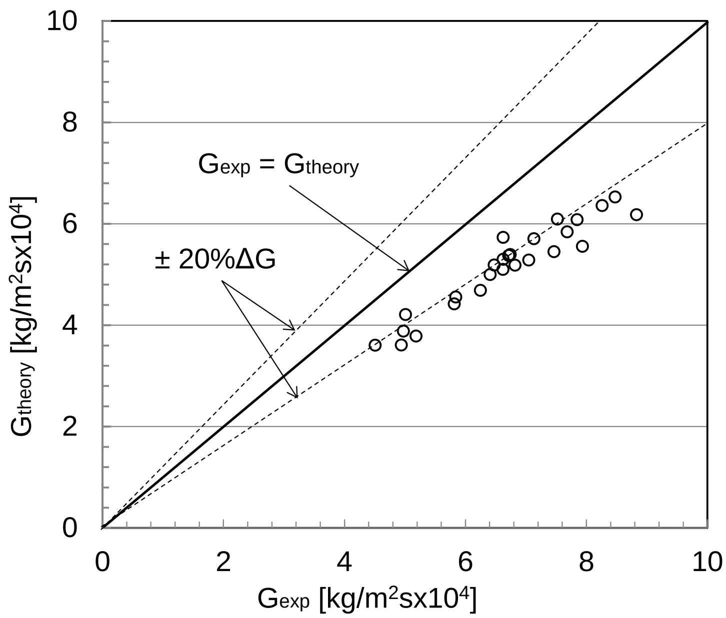

Figure 6. Comparison of HEM predictions with experimental data

6.2 HNEM Model Results

When comparing the HNEM predilection of choking mass flux were compared with the simulated SG crack data, a large improvement is also evident as shown in Figure 7. On average, the predictions are within 10% closer to the experimental values. This shows that applying thermal non-equilibrium assumptions improves the critical mass flux predictions for simulated SG cracks. It is impossible to compare the predicted exit pressures in the current study, however it is evident that thermal non-equilibrium delays flashing and increases the two-phase pressure drop. Also, with the shortened channel length in the present study, flashing is predicted to occur at the exit of the channel in all cases. While from a modeling perspective this was expected, the actual vaporization process in subcooled flashing flows through short narrow channels is up for debate.

It is noticed that the HNEM model better predicts the entrance losses as well as the single-phase frictional pressure drop when compared to the HEM. However, the model obviously predicts flashing to occur further downstream than the experimental estimate of flashing location. Neither model is able to capture the characteristics of the two-phase pressure drop. Both models over predict the exit pressures, however at the highest subcoolings where flashing occurs at the exit, the critical pressure ratio is well predicted. This observation implies that the single phase liquid region may in fact be well predicted in any model using the homogeneous mixture assumptions.

7. CONCLUSIONS

The ability to estimate the leak rates from the through-wall cracks in the steam generator tube is important in terms of radiological source terms and overall operational management of steam generators. A literature survey showed that there are few data sets available on crack geometries related to steam generator tubing. An experimental program was carried out measuring subcooled flashing flow rate through well-defined simulated crack geometries of length 1.3 mm and with $L/D < 2.5$. The crack geometries were first characterized by hydraulic testing and the choking flow tests were carried out for pressures up to 7 MPa and for different subcooling ranging from 24.7C to 50.4 C. The data indicated that as subcooling and stagnation pressure increases, the flashing discharge rate also increases. Both HEM and HNEM were developed to predict the flashing flow in steam generator tube crack. The choking mass flux predictions from HEM under-predicted the data as low as 27%. The prediction from HNEM agreed well within 10% of experimental data for choking discharge rates from such geometries, showing that the thermal non-equilibrium effects are more predominant for the shot length channels

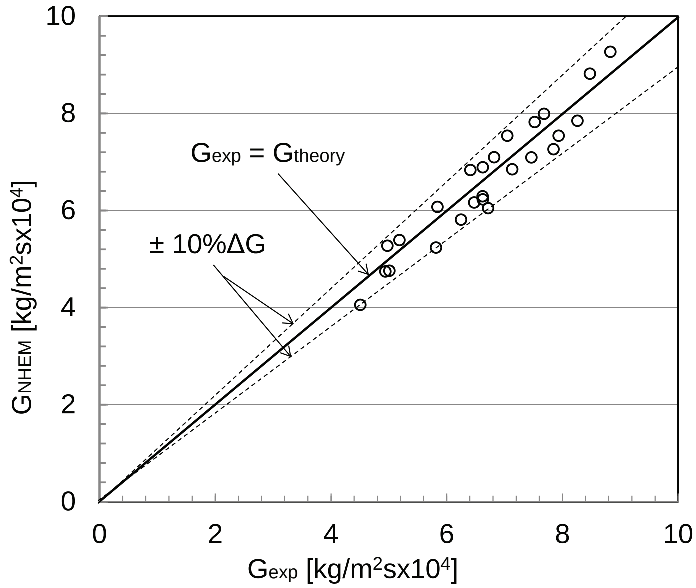

Figure 7. Comparison of HNEM predictions with experimental data

NOMENCLATURE

a	speed of sound (m/s)
C_d	discharge coefficient
d, D	diameter (m]
f	friction factor
g	gravitational acceleration (m/s^2)
G	mass flux (kg/m^{2}s)
h	enthalpy (J/kg)
h_{fg}	latent heat of vaporization (J/kg)
k	conductivity (W/m^{o}C)
L	crack length (m]
m	mass flow rate (kg/s)
P, p	pressure (Pa)
Re	Reynolds number
T	temperature (K or ^{o}C)
s	entropy (J/kg·^{o}C)
t	time (s)
U, u	velocity (m/s)
v	specific volume (m^3/kg)
x	thermodynamic quality
z	axial coordinate (m)

Subscripts

0	stagnation
a	speed of sound
ave	average
b	back pressure
c	critical, choking
cond	condensation
e	entrance
e	exit
eq	equilibrium
exp	experimental
f l	flashing
f	fluid, liquid
fg	difference of vapor-liquid
g	gas or vapor phase
h	hydraulic
HEM	homogeneous equilibrium model
HNEM	homogeneous non-equilibrium model
l	liquid
o	outside, stagnation
r	ratio
s	isentropic
sat	saturation
t	throat
up	upstream
v	vapor

Greek Symbols

α	void fraction
γ	isentropic exponent
Δ	differential
η	pressure ratio
μ	dynamic viscosity (kg/m·s)
ρ	density (kg/m^3)
ρ	density (kg/m^3)
Σ	depressurization rate (Pa/s)
σ	surface tension (N/m)
τ	relaxation time (s)

ACKNOWLEDGMENTS

The work was supported by Canadian Nuclear Safety Commission.

REFERENCES

1. S. Majumdar, "Prediction of structural integrity of steam generator tubes under severe accident conditions," *Nuclear Engineering Design*, **194**, pp. 31-55 (1999).
2. A.R. Vaia, J. M. Stevens and P.J. Prabhu, "Laboratory examination of pulled steam generator tube with free span axial ODSCC," *12th International Conference On Environmental Degradation of*

Materials in Nuclear Power Systems, Salt Lake City, Utah, Minerals, Metals and Materials Society, pp. 1113-1123 (2005).

3. E. Fuller, “Steam Generator Integrity Assessment Guidelines Revision 2” Non-Proprietary Version1012987, Final Report. EPRI Technical Report TR-1012987 (2006).
4. R.F. Keating, P. Hernalsteen and J.A. Begley, “Burst pressure correlation for steam generator tubes with throughwall axial cracks,” Electric Power Research Institute, Palo Alto, California, EPRI Technical Report TR-105505 (1955).
5. P.J. Kichirka, M. Blaszkiewicz, W.A.Byers and G. Pierini “Oconee 2 Steam Generator Tube Examination,” EPRI Technical Report TR-106863 (1997).
6. R.E. Henry and H.K. Fauske, “Two-phase critical flow at low qualities, Part I: experimental; Part II Analysis,” *Nuclear Science and Engineering*, **41**, pp. 79-99 (1970).
7. R.E. Henry and H.K. Fauske, “The two-phase critical flow of one-component mixtures in nozzles, orifices, and short tubes,” *Journal of Heat Transfer*, **93**, pp. 179-187 (1971).
8. R. Henry, “The two-phase critical discharge of initially saturated or subcooled liquid,” *Nuclear Science and Engineering, 41*, 336-342 (1970).
9. C. N. Amos and V. E. Schrock, "Two-phase critical flow in slits," *Nuci. Sci. Eng*., **88**, pp. 261-274 (1984).
10. S. Pagan, X. Duan, M.K. Kozluk, B. Mills and G. Goszczynski, “Characterization and structural integrity tests of ex-service steam generator tubes at Ontario Power Generation,” *Nuclear Engineering Design*, **223**, pp. 477-483 (2009).
11. Westinghouse Electric Corporation, “Burst Pressure correlation for steam generator tubes with through-wall axial cracks,” EPRI, Palo Alto, Report, EPRI TR-105505 (1977).
12. S.T. Revankar and B. Wolf, “Probabilistic assessment of leak rates through steam generator tubes,” Final Report to Canadian Nuclear Safety Commission, PU/NE-10-06 (2010).
13. C. Lackmé, “Thermodynamics of Critical Two-Phase Discharge from Long Pipes of Initially Subcooled Water”, *Heat Transfer in Nuclear Safety Reactors*, pp. 391-407 (1980).
14. M. Alamgir and J.H. Lienhard, “Correlation of pressure undershoot during hot water depressurization,” ASME *Journal of Heat Transfer*, **103**, pp. 52-73 (1981).
15. S. Levy, “Prediction of two-phase critical flow rate,” *J. of Heat Transfer*, **87**(1), pp. 53–58 (1965).
16. E. G. Bauer, G.R. Houdayer and H.M. Sureau, “A Non-Equilibrium Axial Flow Model And Application To Loss-of-Coolant Accident Analysis: The Clystere System Code,” In *OECD/NEA Specialists’ Mtg. on Transient Two-Phase Flow*, Toronto, August. Vol. 1, pp. 429-458 (1976).
17. S.Y. Lee and V.E. Schrock, 1990, “Critical Two-Phase Flow in Pipes for Subcooled Stagnation States With a Cavity Flooding Incipient Flashing Model,” *J. of Heat Transfer*, **112**, pp. 1031-1040 (1990).
18. S. Levy and D. Abdollahian, “Homogeneous Non-Equilibrium Critical Flow Model,” *International Journal of Heat and Mass Transfer*, **25**(6), pp.759–770 (1982).
19. S. Kaizerman, E. Wacholder and E. Elias, “Characteristic Analysis Of Inhomogeneous, Nonequilibrium, Two-Phase Flows Using The Drift-Flux Model,” *Nucl. Sci. and Eng.,* **84**(2), pp.168–173 (1983).